JACS
JOURNAL OF THE AMERICAN CHEMICAL SOCIETY
Communication
pubs.acs.org/JACS

Staged Self-Assembly of Colloidal Metastructures

Qian Chen,[†] Sung Chul Bae,[†] and Steve Granick*[,†,‡,§]

[†]Department of Materials Science and Engineering, [‡]Department of Physics, and [§]Department of Chemistry, University of Illinois, Urbana, Illinois 61801, United States

Supporting Information

ABSTRACT: We demonstrate sequential assembly of chemically patchy colloids such that their valence differs from stage to stage to produce hierarchical structures. For proof of concept, we employ ACB triblock spheres suspended in water, with the C middle band electrostatically repulsive. In the first assembly stage, only A−A hydrophobic attraction contributes, and discrete clusters form. They can be stored, but subsequently activated to allow B−B attractions, leading to higher-order assembly of clusters with one another. The growth dynamics, observed at a single particle level by fluorescence optical microscopy, obey the kinetics of stepwise polymerization, forming chains, pores, and networks. Between linked clusters, we identify three possible bond geometries, linear, triangular, and square, by an argument that is generalizable to other patchy colloid systems. This staged assembly strategy offers a promising route to fabricate colloidal assemblies bearing multiple levels of structural and functional complexity.

The majority of self-assembly strategies currently involve a single stage, wherein the particle−particle interaction energies are given from the start.[1] In this approach, all information needed to direct assembly must be encoded into the building blocks from the beginning. As an example of how this limits possibilities, consider a hypothetical design goal: a porous colloidal sheet with two levels of complexity (see Figure S1)[2] whose hierarchical porous structure, if it could be assembled, might serve as catalyst support, photonic crystal, or substrate for specific host−guest interactions.[1d,3] In a single-stage assembly scheme, one would require octahedral building blocks with attraction sites located precisely at each of the six protruding ends (Figure S1). To form these complicated colloids would pose a formidable synthetic challenge.[4] In contrast, if one decomposes the assembly into two stages, one can employ, as the primary building block, triblock colloidal spheres which are simple to synthesize[1d,5] (Figure S1). This strategy, demonstrated in the organization of biological molecules,[6] synthetic polymers,[7] DNA architecture,[8] and nanocrystals,[9] has been mentioned in the colloid field,[10] but is insufficiently developed.

To implement staged assembly of colloids, the needed asymmetric triblock spheres with patches A and B at the two poles, and a repulsive middle C, can be fabricated in high fidelity and monodispersity following a method developed recently in this lab.[1d,5b] We select negatively charged polystyrene particles as the parent particles because their density allows the formation of three-dimensional small clusters without prohibitive sedimentation.[11] We refer to an attractive contact as a "bond." We design patches A and patch B as both of them hydrophobically attractive, but with different patch sizes (see Figure 1a). This difference enables the sequential activation of the bonds.

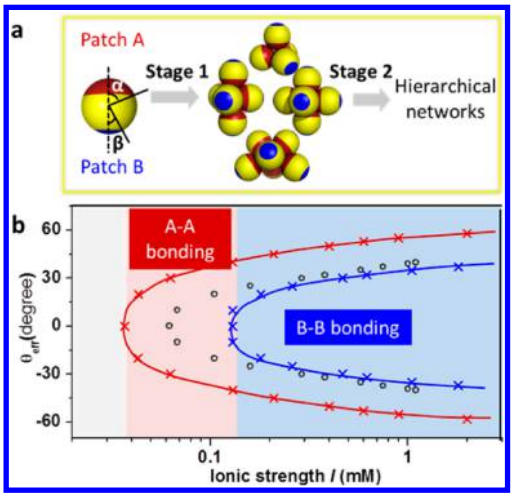

Figure 1. Schematics of staged self-assembly. (a) ACB triblock spheres (α, half opening angle for A patch, is 60°, β for B patch is 40°) can activate A−A bonds first to form small clusters, including tetrahedron, pentamer, octahedron, and capped trigonal bipyramid (CTBP), and then initiate B−B bonds to grow into hierarchical networks. (b) Theoretical calculation (see Supporting Information (SI) for details) showing the effective patch size of A−A bonds (red crosses), B−B bonds (blue crosses), and A−B bonds (gray circles). A−A bonds can be turned on in a window of low ionic strength I (red regime), while B−B bonds can be activated later at an elevated ionic strength (blue regime).

This scheme simplifies the design of building blocks and also guides the assembly selectively along a pathway toward the lowest energy state while avoiding kinetic traps. In particular, since hydrophobic attraction is short-ranged relative to particle size (1 μm), the thermodynamically stable structures are those with the most bonds: the network structures with the most A−A and B−B bonds. Staged assembly minimizes kinetic formation of A−B bonds, which would be less stable but might present kinetic bottlenecks. For example, using the same ACB building blocks, we also did control experiments where we

Received: April 10, 2012
Published: June 25, 2012

   dx.doi.org/10.1021/ja303434d | J. Am. Chem. Soc. 2012, 134, 11080−11083

increased ionic strength to the final value in a single shot. Colloidal assemblies formed but their structures, which included A−B bonds, were messy. Consequently, the metastructure clusters were more polydisperse and the final structures were less clean in geometrical shape (see Figure S1).

Our experimental handle to achieve staged assembly is ionic strength, to which the two patches respond distinctively. The total pairwise interaction between adjacent ACB colloids, the sum of hydrophobic attraction and electrostatic repulsion, ranges from repulsive to attractive depending on their mutual orientation. We describe this dependence as an effective patch size θ_{eff}, namely, the effective attractive patch size the neighboring particles see for each other. Calculation quantifies that A−A bonds possess a significant θ_{eff} value at lower ionic strength window than B−B (see Figure 1b, Figure S2 and discussion in SI). This indicates that one can first activate solely A−A bonds, then subsequently increase ionic strength to attach dangling B sites for secondary assembly. The hydrophobically attractive bond, with a strength of 7 k_BT suggested by our earlier study,[11] is strong enough to bias bonds to form but still weak enough to allow correction of misaligned bonds to maximize A−A or B−B bonds at each stage.

Our experiment validates this idea. At the first stage where I = 1.2 mM (NaCl), triblock spheres form small three-dimensional clusters ("metastructures"),[12] the same structures formed by AC Janus spheres with one sole type of attractive bond.[11] These clusters are stable 20 min after salt addition, with a cluster size distribution peaked at tetrahedral shapes (see Figure S3 and Movie S1). Note that the shape of this distribution depends on both the initial particle concentration and patch size design. When B−B bonds are triggered later, clusters recognize each other in three different bond types: the linear, the triangular, and the right angle conformations illustrated in Figure 2a. These three bond types further tile into a family of unprecedented porous networks (see Figures 2b, S4, and Movie S2). The self-assembly is basically a planar arrangement of small clusters, because individual clusters are dense enough to sediment to a thin near-surface region, within which the particle volume fraction is typically around 30%. The novelty is the structural, and potentially functional hierarchy: at each site of the pores are small clusters, not the primary triblock spheres. In other words, the products of the first stage serve as the secondary building blocks for the second stage. Three-dimensional assemblies can be expected to follow a similar staged assembly scheme.

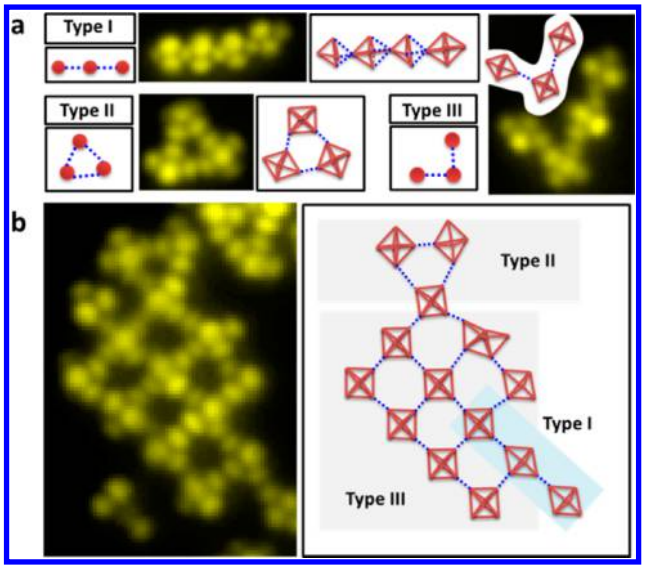

Figure 2. Fluorescence microscopy images of assemblies formed at I = 5 mM (NaCl). The yellow spheres are 1 μm sized ACB triblock spheres. Schematic diagrams distinguish between bonds formed in the first (red solid lines) and second (blue dotted lines) stages of assembly. (a) Three bond types are shown: linear, triangular, and right angle conformations. Red spheres denote a cluster; blue lines denote bonds between clusters. (b) An illustrative network structure combining the three bond types.

The convergence into just three primary bond geometries between clusters, in spite of the diversity of the clusters themselves,[11] is striking. This is because each cluster can be conceived as a larger patchy particle decorated with multiple attraction sites, the dangling B patches, at the protruding ends. Therefore, the subsequent bonding geometry of this "patchy particle" depends on its geometrical shape. We have analyzed the fluorescence images of a statistically significant collection of the final assemblies and, for each cluster shape, have identified and quantified the relative abundance of the three bond types (Table 1). Entropy arguments presented in the next paragraph can probably explain their relative stability, but no quantitative explanation of this is offered at this time. Here we emphasize that the relative abundance of bond types for a given cluster shape can give a rule of thumb to guide more such design in the future: for example, if the final "square"-like network structure were desired, we could start with octahedra as the secondary building block, as this bears the desired right-angle bond type.

Table 1. Connection Schemes When Small Clusters Link Together[a]

cluster	bond type i	$P_{i,N}$	bond geometry
N=4		(0.78)	
		(0.03)	
		(0.19)	
N=5		(0.45)	
		(0.15)	
		(0.40)	
N=6		(0.27)	
		(0.03)	
		(0.70)	
N=6		(0.67)	
		(0.33)	

[a]The bonds formed at the first stage are shown as red lines, the second stage as blue lines. All the schemes are deduced from statistical counting based upon experimental observation of final assemblies. In the "$P_{i,N}$" column, the length of the grey bars shows relative probability to find one bond type at a cluster size of N. For each cluster shape, the statistics is based upon manual counting of around 100 such clusters.

Now that we view the small clusters as polyvalent structural units, each of the sites on the cluster capable of bonding with

dx.doi.org/10.1021/ja303434d | J. Am. Chem. Soc. 2012, 134, 11080−11083

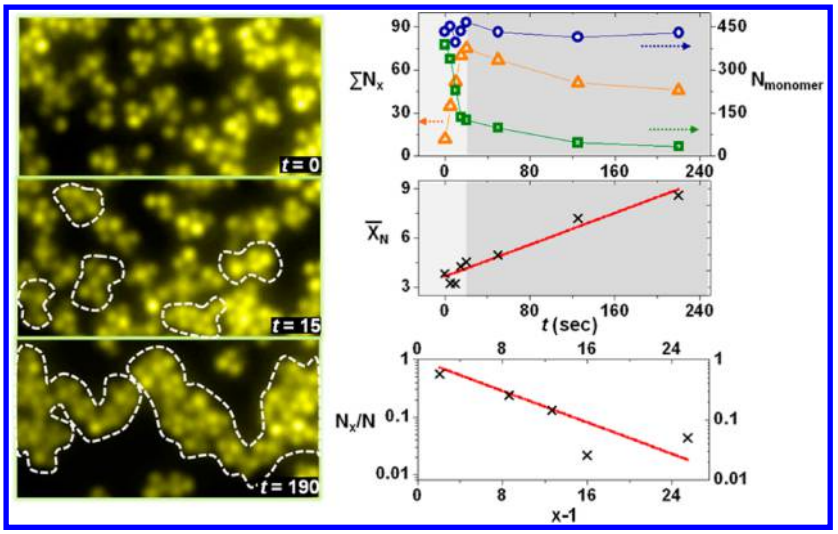

Figure 3. Step-growth polymerization from small clusters. (Left) A time series of fluorescence optical images. Elapsed time in seconds is shown in the inset. The size of connected islands (x-mers of clusters) is highlighted by dotted lines. (Right) Quantification of the distribution of x-mers at different times, showing agreement with step-growth polymerization. In the top graph, blue circles are the total number of component small clusters (monomers), green squares the number of free monomers, and orange triangles the number-average of x-mers ($\sum N_x$). See SI for details.

another cluster according to known connection schemes, we can describe their assembly in a simpler language. The bonding force, although it resides in distinct locations distributed over the surface of the metastructure units, originates in hydrophobic attraction, which is not directional.[1d,11] Assembly is determined by the coordinated effects of collision frequency and orientation matching. This physical situation resembles the classical step-growth polymerization mechanism[13]—specifically, no initiator is needed to start the reaction and the reaction rates are the same at every growth step (see Figure 3). To make this quantitative for the system studied here, notice that the total number of small clusters does not change, which means it is a closed system, and that we observe at short times the rapid loss of free clusters, the analogue of polymerization "monomers." The number-average degree of polymerization grows in proportion to time and in the distribution of "polymers" the abundance of those containing a number x of linked clusters decreases exponentially with $(x - 1)$. Pointing toward the generality of this physical process, notice that similar growth laws were observed recently for nanoparticle assembly.[14] All of these are known features of textbook step-growth polymerization of small molecules. It seems that quantitative predictions regarding a broad class of related systems should be possible, as the underlying assumptions are rather simple and easy to satisfy.

We do realize a limitation of our current design of using A–A and B–B bonds, as A–B bonds occasionally emerge as a side reaction during the second assembly stage. Perhaps truly orthogonal attraction types such as biological recognition[1a] can be incorporated later to exclude that side reaction, as the challenging aspect is how to introduce orthogonal attractions onto the surface of the same colloidal particle. A second limitation is the distribution of product sizes produced by step-growth polymerization. One can try to find ways to stabilize and fractionate these secondary building blocks, as the colloidal analogue of living polymerization,[15] which is known for producing products of uniform size, is not yet known. A third limitation is that data in this paper are limited to staged self-assembly controlled by stepwise change of ionic strength. However, the same strategy should apply to other triggers of staged assembly, such as pH, temperature, and chemical reactions. There are many ways to generalize the main idea: that staged assembly biases the kinetic pathway by controlling intermediate structures at different steps.

■ ASSOCIATED CONTENT

Supporting Information

Experimental sections, supplementary discussions, including Figures S1–S4, and Supplementary movies Movie S1, S2. This material is available free of charge via the Internet at http://pubs.acs.org.

■ AUTHOR INFORMATION

Corresponding Author

sgranick@illinois.edu

Notes

The authors declare no competing financial interest.

■ ACKNOWLEDGMENTS

This work was supported at the University of Illinois by the U.S. Department of Energy, Division of Materials Science, under Award DE-FG02-07ER46471 through the Frederick Seitz Materials Research Laboratory at the University of Illinois at Urbana–Champaign.

■ REFERENCES

(1) For example: (a) Hormoz, S.; Brenner, M. P. *Proc. Natl. Acad. Sci. U.S.A.* **2011**, *108*, 5193. (b) Sacanna, S.; Irvine, W. T. M.; Chaikin, P. M.; Pine, D. J. *Nature* **2010**, *464*, 575. (c) Lu, P. J.; Zaccarelli, E.; Ciulla, F.; Schofield, A. B.; Sciortino, F.; Weitz, D. A. *Nature* **2008**, *453*, 499. (d) Chen, Q.; Bae, S. C.; Granick, S. *Nature* **2011**, *469*, 381.

(2) O'Keeffe, M.; Peskov, M. A.; Ramsden, S. J.; Yaghi, O. M. *Acc. Chem. Res.* **2008**, *41*, 1782. The structure is one layer of the uniform tiling net with a symbol of "cab" in the Reticular Chemistry Structure Resource (RCSR) Database.

(3) (a) Su, B.-L.; Sanchez, C.; Yang, X.-Y. *Hierarchically Structured Porous Materials: From Nanoscience to Catalysis, Separation, Optics, Energy, and Life Science*; Wiley-VCH: Weinheim, 2012; pp 55–129. (b) Galisteo-López, J. F.; Ibisate, M.; Sapienza, R.; Froufe-Pérez, L. S.; Blanco, Á.; López, C. *Adv. Mater.* **2011**, *23*, 30.

(4) Kraft, D. J.; Vlug, W. S.; van Kats, C. M.; van Blaaderen, A.; Imhof, A.; Kegel, W. K. *J. Am. Chem. Soc.* **2009**, *131*, 1182.
(5) (a) Glotzer, S. C.; Solomon, M. *Nat. Mater.* **2007**, *6*, 557. (b) Chen, Q.; Diesel, E.; Whitmer, J.; Bae, S. C.; Luijten, E.; Granick, S. *J. Am. Chem. Soc.* **2011**, *133*, 7725.
(6) Keizer, H. M.; Sijbesma, R. P. *Chem. Soc. Rev.* **2005**, *34*, 226.
(7) Ikkala, O.; ten Brinke, G. *Chem. Commun.* **2004**, 2131.
(8) He, Y.; Ye, T.; Su, M.; Zhang, C.; Ribbe, A. E.; Jiang, W.; Mao, C. *Nature* **2008**, *452*, 198.
(9) (a) Miszta, K.; de Graaf, J.; Bertoni, G.; Dorfs, D.; Brescia, R.; Marras, S.; Ceseracciu, L.; Cingolani, R.; van Roij, R.; Dijkstra, M.; Manna, L. *Nat. Mater.* **2011**, *10*, 872. (b) Zhang, S.; Li, Z.; Samarajeewa, S.; Sun, G.; Yang, C.; Wooley, K. L. *J. Am. Chem. Soc.* **2011**, *133*, 11046.
(10) (a) Onoe, H.; Matsumoto, K.; Shimoyama, I. *Small* **2007**, *3*, 1383. (b) Jia, X.-X.; Li, Z.-W.; Sun, Z.-Y.; Lu, Z.-Y. *J. Phys. Chem. B* **2011**, *115*, 13441.
(11) Chen, Q.; Whitmer, J.; Jiang, S.; Bae, S. C.; Luijten, E.; Granick, S. *Science* **2011**, *331*, 199.
(12) Agarwal, U.; Escobedo, F. A. *Nat. Mater.* **2011**, *10*, 230.
(13) Flory, P. J. *Principles of Polymer Chemistry*; Cornell University Press; Ithaca, NY, 1953.
(14) Liu, K.; Nie, Z.; Zhao, N.; Li, W.; Rubinstein, M.; Kumacheva, E. *Science* **2010**, *329*, 197.
(15) Szwarc, M. *Nature* **1956**, *178*, 1168.